JOURNAL OF THE ROYAL SOCIETY Interface

J. R. Soc. Interface (2010) **7**, 143–152
doi:10.1098/rsif.2009.0102
Published online 27 May 2009

Ant antennae: are they sites for magnetoreception?

Jandira Ferreira de Oliveira[1,2,*], Eliane Wajnberg[2], Darci Motta de Souza Esquivel[2], Sevil Weinkauf[1], Michael Winklhofer[3] and Marianne Hanzlik[1]

[1]*Fakultät für Chemie—FG Elektronenmikroskopie—Technische Universität München, Lichtenbergstr. 4, 85747 Garching, Germany*
[2]*Departamento de Física Aplicada/CBPF, R. Xavier Sigaud 150, Urca, CEP, 22290-180 Rio de Janeiro, Brazil*
[3]*Department of Earth and Environmental Sciences, Ludwig–Maximilians-Universität, Theresienstrasse, 41, 80333 Munich, Germany*

Migration of the *Pachycondyla marginata* ant is significantly oriented at 13° with respect to the geomagnetic north–south axis. On the basis of previous magnetic measurements of individual parts of the body (antennae, head, thorax and abdomen), the antennae were suggested to host a magnetoreceptor. In order to identify Fe^{3+}/Fe^{2+} sites in antennae tissue, we used light microscopy on Prussian/Turnbull's blue-stained tissue. Further analysis using transmission electron microscopy imaging and diffraction, combined with elemental analysis, revealed the presence of ultra-fine-grained crystals (20–100 nm) of magnetite/maghaemite (Fe_3O_4/γ-Fe_2O_3), haematite (α-Fe_2O_3), goethite (α-FeOOH) besides (alumo)silicates and Fe/Ti/O compounds in different parts of the antennae, that is, in the joints between the third segment/pedicel, pedicel/scape and scape/head, respectively. The presence of (alumo)silicates and Fe/Ti/O compounds suggests that most, if not all, of the minerals in the tissue are incorporated soil particles rather than biomineralized by the ants. However, as the particles were observed within the tissue, they do not represent contamination. The amount of magnetic material associated with Johnston's organ and other joints appears to be sufficient to produce a magnetic-field-modulated mechanosensory output, which may therefore underlie the magnetic sense of the migratory ant.

Keywords: ant antennae; iron oxides; Johnston's organ; magnetoreception

1. INTRODUCTION

Geomagnetic sensitivity and magnetic orientation behaviour have been intensively studied in a range of animals across all major groups (Wiltschko & Wiltschko 1995; Gould 2008; Lohmann *et al.* 2008), but the mechanisms by which animals can perceive the geomagnetic field and transduce it into a nerve signal remain to be identified. Current research into magnetoreception is driven mainly by two hypotheses that rely on two fundamentally different but not mutually exclusive physical principles. The radical-pair hypothesis assumes a special class of molecules that undergo magnetically anisotropic chemical reactions as the basis for the magnetic compass sense (Ritz *et al.* 2000, 2004; Maeda *et al.* 2008). Migratory birds, for example, appear to have the radical-pair mechanism for the inclination compass and additionally a magnetite-based system for the navigational map (Wiltschko *et al.* 2008). The magnetite hypothesis postulates the involvement of ferrimagnetic material (e.g. biogenic magnetite) coupled to mechanosensitive structures so as to transmit the information on the geomagnetic field in the form of a torque or force into the nervous system (Kirschvink & Gould 1981; Shcherbakov & Winklhofer 1999; Davila *et al.* 2003, 2005; Ferreira *et al.* 2005). The first step towards confirming the magnetite hypothesis is to demonstrate the presence of magnetic nanoparticles in or around innervated structures in animal tissues (Diebel *et al.* 2000; Fleissner *et al.* 2003).

The discovery of magnetotactic bacteria (Blakemore 1975) defined a milestone for the magnetite hypothesis. Intracellular chains of biomineralized single-domain (SD) magnetite crystals arranged parallel to the motility axis of these micro-organisms make the bacteria orient themselves passively along the geomagnetic field lines, taking them to nutrient-rich and oxygen-poor environments.

Magnetic particles were found in specific tissues or in extracts of body parts of animals (O'Leary *et al.* 1981; Vilches-Troya *et al.* 1984; Mann *et al.* 1988; Walker *et al.* 1997; Diebel *et al.* 2000; Hanzlik *et al.* 2000), but only in the rainbow trout *Oncorhynchus mykiss* (Walker *et al.* 1997) and the homing pigeon (Hanzlik *et al.* 2000; Fleissner *et al.* 2003) the magnetite found

*Author and address for correspondence: Departamento de Física Aplicada/CBPF, R. Xavier Sigaud 150, Urca, CEP, 22290-180 Rio de Janeiro, Brazil (jandiuff@cbpf.br).

Received 18 March 2009
Accepted 21 April 2009

seems to have a direct neural connection. Behavioural studies with social insects such as termites, bees and ants have shown orientational and navigational responses to the geomagnetic field (Wiltschko & Wiltschko 1995; Vacha 1997), and a magnetoreceptor system based on superparamagnetic (SPM) magnetite particles in the abdomen was proposed for honeybees (Gould *et al.* 1978; Hsu *et al.* 2007).

Most of the ant species are known primarily for being 'chemical' animals. Pheromones, the main mediator of communication in these animals, are used by a forager to transfer information to the other workers about food sources or to warn the ants about an imminent attack. Landmarks and polarized light are important for homing. The influence of the geomagnetic field in ant species was reported for the species *Formica pratensis* (Çamlitepe *et al.* 2005), *Solenopsis invicta* (Anderson & Vander Meer 1993), *Formica rufa* (Çamlitepe & Stradling 1995) and *Atta colombica* (Riveros & Srygley 2008).

Migration of the ant *Pachycondyla marginata* is significantly oriented at a 13° angle with respect to the geomagnetic north–south axis (Acosta-Avalos *et al.* 2001). Magnetic measurements on individual parts of the body (head, antenna, abdomen and thorax) showed that the strongest magnetic signal comes from the antennae (Wajnberg *et al.* 2004). In addition, behavioural experiments carried out with the *Myrmica ruginodis* ant showed that the antennae respond to magnetic fields with the pedicel being the most influenced part (Vowles 1954). Based on these results and considering the still-emerging knowledge on the magnetic material in animals and the preliminary magnetic data on the *P. marginata* ant (Acosta-Avalos *et al.* 1999; Wajnberg *et al.* 2000, 2004), we used light microscopy (LM) and transmission electron microscopy (TEM) in this study to identify a possible magnetic sensor in the antennae, a promising sensory organ for magnetoreception.

2. MATERIAL AND METHODS

Pachycondyla marginata workers were collected in the act of foraging in the region of Campinas, São Paulo, Brazil, in September 2006 (Sep06) and May 2007 (May07). The animals were transported alive in boxes containing soil from the nest and its neighbourhood (Sep06) and free of soil (May07). Some of the ants died and were separated only for extraction procedures. For electron microscopic measurements, alive ants were kept in the freezer until no movement was observed. The ants were divided into head with antenna, thorax and abdomens, put separately in ethanol 70 per cent and sonicated for 5 min to eliminate soil particles that could be attached to the cuticle surface.

2.1. Magnetic extraction

For magnetic extractions, antennae and heads of 47 (Sep06) and 50 (May07) individuals were separated from each other, and the procedure in Acosta-Avalos *et al.* (1999) was followed. Ant body parts were macerated in the presence of 5 per cent sodium hypochlorite (NaOCl) solution (Reagen, Brazil), and the cuticle was removed. Approximately equal amounts of each sample were placed in 1.5 ml Eppendorf tubes, more NaOCl solution was added to half fill the tubes and they were left overnight at 4°C. The tubes were centrifuged at 15 700g for 8 min to pellet the insoluble material. The supernatant consisting of dissolved organic matter was discarded, and a further 0.75 ml of NaOCl solution was added to each pellet. After resuspending the pellets both manually and using ultrasonic vibration for 15 min, the material was subjected to magnetic concentration by placing a strong (Sm-Co) magnet on the lateral wall (not the bottom) of the tubes for 10 min. The resultant red/orange pellet was partially removed with the supernatant, and successive magnetic concentrations were performed to reduce the pellet to a minimum. The same centrifugation, sonication and magnetic concentration procedures were applied to two soil samples. The magnetic concentration of soil resulted in a black concentrated material on the wall of the Eppendorf tube, but this process did not remove all magnetic content of the pellet. The magnetic concentrate and the resuspended pellet, called soil solution, were kept.

After several NaOCl centrifugation steps, chloroform was used to remove fat, with washing procedures similar to the one described earlier. This process was repeated until most of the organic matter and fat had been digested and the orange precipitate did not change its colour. The pellet was washed in distilled water and precipitated by centrifugation. Just before the measurement, the material was sonicated and again magnetically concentrated, and the resulting material of each part on the wall (not observed visually) was dropped onto a TEM grid covered with a carbon film. In the antennae sample, even the pellet was not observed visually. Therefore, the solution was stirred for several minutes with a magnetic finger and the adhering drop was air-dried on a TEM grid. All body parts from Sep06 samples were measured, while only antennae from May07 samples were analysed.

Bright field images and selected area electron diffraction (SAED) patterns were taken at 100 kV with a transmission electron microscope Jeol JEM100 CX.

2.2. Turnbull's/Prussian blue reaction and LM

To locate regions containing iron particles focusing on magnetite, Prussian blue (PB for Fe^{III}) and Turnbull's blue (TB for Fe^{II}) reagents were applied for 10 min to serial histological sections (10 μm thickness, longitudinal (L) or transversal (T) to the antennae) of half heads with antennae or only antennae (total : 8). In the presence of HCl, Fe^{III} and Fe^{II} react with potassium ferrocyanide and ferricyanide, respectively, to yield the dark blue ferric ferrocyanide:

$$\begin{aligned} \mathrm{PB}: & \mathrm{K_4[Fe^{II}(CN)_6] + Fe^{III}Cl_3} \\ & \leftrightarrow \mathrm{KFe^{III}Fe^{II}(CN_6) + 3KCl}, \\ \mathrm{TB}: & \mathrm{K_3[Fe^{III}(CN)_6] + Fe^{II}Cl_2} \\ & \leftrightarrow \mathrm{KFe^{II}Fe^{III}(CN_6) + 2KCl}. \end{aligned}$$

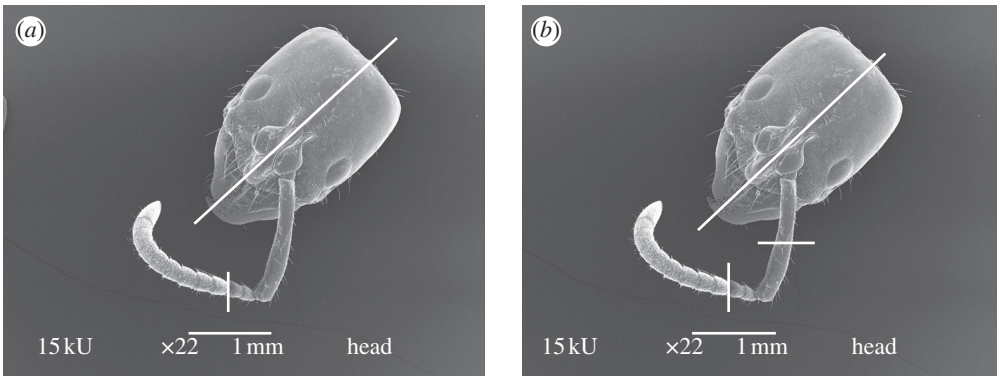

Figure 1. Scanning electron microscopy micrograph of head with antenna of *P. marginata* ant showing the cutting planes (white lines). (*a*) Sep06 preparation, two divisions: one dividing the head into two equal parts and the other at the third/fourth segment joint and (*b*) May07 preparation, three divisions: the first and third one as in (*a*), the second at the middle of the scape. The cut direction was transverse or longitudinal through each antenna segment.

The samples were immediately inspected and, when possible, the presence of Fe regions in consecutive slices of the same sample or in the same region of another sample was verified to discard the iron of contaminant soil particles. Magnetite is the iron oxide most frequently found in animals and, owing to its magnetic properties, it is also desirable from the point of view of magnetoreception. Stoichiometric magnetite consists of one-third ferrous and two-thirds ferric iron, but since ferric iron also occurs in iron storage proteins, we consider the ferrous iron reaction (TB) to be more appropriate for the detection of magnetite. The PB was used at the same time as a control.

2.3. Thin sectioning

Ant antennae are elbow-shaped and divided into segments: the scape, the longest one connected to the head, followed by the pedicel and then the other segments that compose the flagellum (figure 1). Before cutting, the flagellum was aligned with the scape providing only one cutting direction, transverse or longitudinal through the whole antenna. A longitudinal cut was performed in the frontal part of the head to facilitate diffusion of the fixatives. Heads with antennae of samples Sep06 and May07 were cut in two or three positions, respectively, as shown in figure 1.

Sep06 sample parts were fixed in cacodylate-buffered 4 per cent paraformaldehyde and 2.5 per cent glutaraldehyde (Karnovsky's fixative) solution for 48 h, while May07 samples were fixed in cacodylate-buffered 2.5 per cent glutaraldehyde solution overnight. Both samples were post-fixed in cacodylate-buffered 1 per cent osmium tetroxide solution for 40 min and 1 h, respectively. The May07 samples were embedded in 2.5 per cent low melting point agarose. Samples were then dehydrated with ethanol, plastic-embedded in SPURR and ultrathin sectioned to 100–200 nm. Selected area electron diffraction patterns and bright field images were taken from one Sep06 sample (third segment to head) and two May07 samples (third segment to scape) at 100 kV with a Jeol 100 CX or at 120 kV with a Jeol 2000 FX equipped with an EDAX Genesis system for X-ray energy dispersive spectroscopy (EDX).

3. RESULTS

The collected soil is red/orange and the magnetic extraction procedure resulted in a black concentrated material on the lateral wall of the tube, close to the magnet position, which appeared as agglomerated particles on TEM (data not shown). Figure 2*a* shows a TEM micrograph of the sample called soil solution in the magnetic extraction section. Energy dispersive spectroscopy analysis of the particles in figure 2*a* revealed the presence of Fe/O, Si/Al/O, Fe/Ti/O and Ti/O particles. Clusters of 14 μm and particles from <200 nm size up to 6 μm were observed.

An orange precipitate appeared at the bottom of the tube in the antenna, head, thorax and abdomen magnetic extractions (Sep06), with the abdomen having the highest amount and the antenna the lowest. The amount of orange precipitate was strongly reduced in May07 samples, and was not observed in the antenna extracts. TEM micrographs of magnetically concentrated particles of head, abdomen and thorax were obtained after the washing procedure, and a thorax image is shown, as an example, in figure 2*b*. Clusters of 14 μm and particles from <100 nm size up to 7 μm were observed. Energy dispersive spectroscopy measurements showed that these particles are composed of Fe/O, Si/Al/O, Ti/O and Fe/Ti/O. Powder diffraction patterns of these particles and of those in the soil solution were taken, and their calculated d-spacings are compared with magnetite in table 1.

The d-spacings of the soil solution are common to many Al/Si/O compounds and Al, Si, O compositions with other elements such as Mn, Na and Ca (American Mineralogist Crystal Structure Database), while the body extract d-spacings indicate the presence of Al/Si/O and iron-containing particles.

Compared with the other body part extracts, a large amount of 50 nm Fe/O particles (figure 3*a*) and a significant decrease in the amount of Si/Al/O particles were observed in the antenna magnetic extracts of the May07 sample. The 50 nm Fe/O particles displayed electron diffraction patterns, as shown in figure 3*b*. The calculated d-spacings of 2.52 Å together with the measured angle of 60° between two directions (i.e. the angle between two crystalline planes) were used to identify the crystal as haematite.

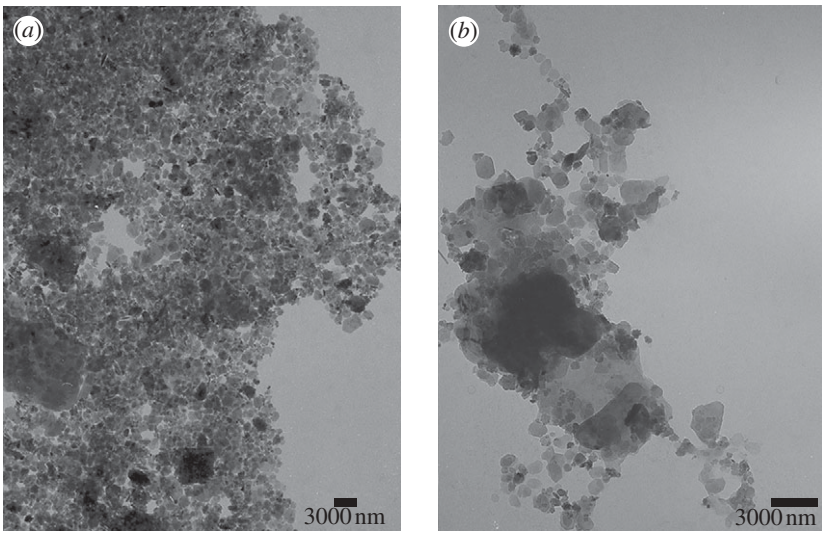

Figure 2. Transmission electron microscopy micrograph of (*a*) soil solution and (*b*) magnetic extracts from thorax of the *P. marginata* ant.

Table 1. Comparison of the experimental lattice distances (*d*), in angstroms (Å), of ant body extracts and soil solution to the known patterns of three iron oxides. (The percentages in parentheses are the relative intensities measured from X-ray powder diffraction and are directly related to the probability that each diffraction point appears in any diffraction pattern. X-ray powder diffraction data were obtained from the Joint Committee for Powder Diffraction Standards (JCPDS) database. The corresponding card numbers in this database are 19-629 for magnetite, 13-534 for haematite and 29-713 for goethite.)

magnetite, *d* (Å)	haematite, *d* (Å)	goethite, *d* (Å)	soil (solution), *d* (Å)	abdomen (Sep06), *d* (Å)	thorax (Sep06), *d* (Å)	head (Sep06), *d* (Å)	antennae (Sep06), *d* (Å)
4.85 (8)		4.18	4.28	4.28	4.28		4.28
	3.67	3.38					
2.97 (30)				3.09		2.97	
	2.69	2.69				2.65	
2.53 (100)	2.51	2.58/2.53					2.53
2.42 (8)		2.48/ 2.45	2.42	2.42	2.42		
	2.23	2.30	2.32			2.32	
	2.20	2.25/2.19	2.14		2.14		
2.01 (20)	2.07	2.09/2.01/1.92				1.97	
1.71 (10)	1.84	1.80/1.77/1.72					
1.62 (30)	1.69/1.63	1.69/1.66/1.60	1.64		1.64		

As soil contaminants can be present in the magnetic extracts, the biogenic origin of single crystals should be proven by their detection within well-preserved embedded tissue. We therefore observed PB/TB reactions in semi-sections by LM to roughly identify sites of iron compounds. Fe^{3+} and Fe^{2+} sites were only observed by LM in the joint of the scape with the head (data not shown).

Ultrathin sectioning and electron microscopy were used to obtain the precise position within the tissue. Transmission electron microscopy bright field images of ultrathin sections showed iron concentrations in several transversal ultrathin sections through the three main antennal joints: pedicel/third segment, scape/pedicel and head/scape, not observed in the semi-sections by LM, probably because the regions were too small to be observed by LM.

Micrographs of the transversal ultrathin sections through the third segment/pedicel joint (figure 4*a*, inset) are shown in figure 4*a*,*b*. In figure 4*a*, an empty knob shows a long sensory process, while the overall EDX spectrum of the particles in figure 4*b* indicated the presence of Fe, Si, Al and O. The region with particles in figure 4*b* is magnified in figure 4*c*. Several diffraction patterns of the iron-containing particles were taken and they indicated the presence of goethite and/or haematite and other iron-containing particles that could not be identified. As an example, the diffraction pattern of the particle indicated by the arrow in figure 4*c* is shown (figure 4*d*). The particles were found inside the epicuticular invagination (Masson & Gabouriaut 1973) or cuticular knobs (Tsujiuchi *et al.* 2007), into which the long sensory process (arrow in figure 4*a*) (Hallberg 1981) from the scolopidia comes.

Iron oxides, alumosilicates, silicates and Ti/O particles were also found in transversal ultrathin sections through the pedicel (P)/scape (S) joint (figure 5*a*, inset). Particles surrounding a cell-like structure were

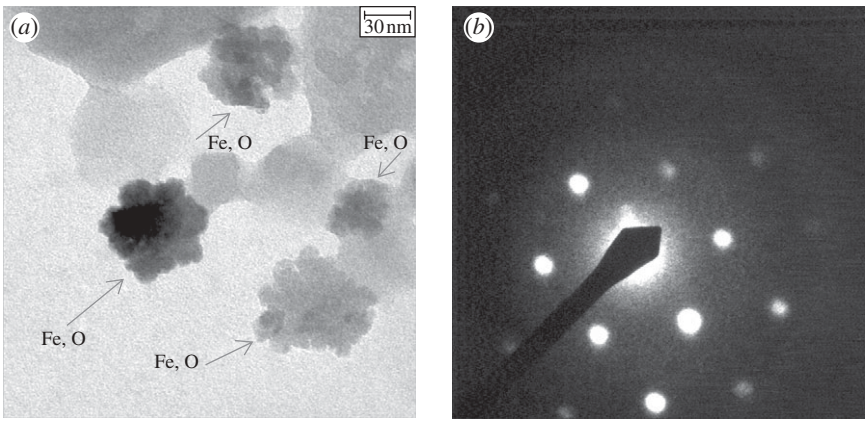

Figure 3. (*a*) Transmission electron microscopy micrograph of 50 nm Fe/O particles in antenna magnetic extracts of the May07 sample, identified as haematite by (*b*) the diffraction pattern of one of the crystals.

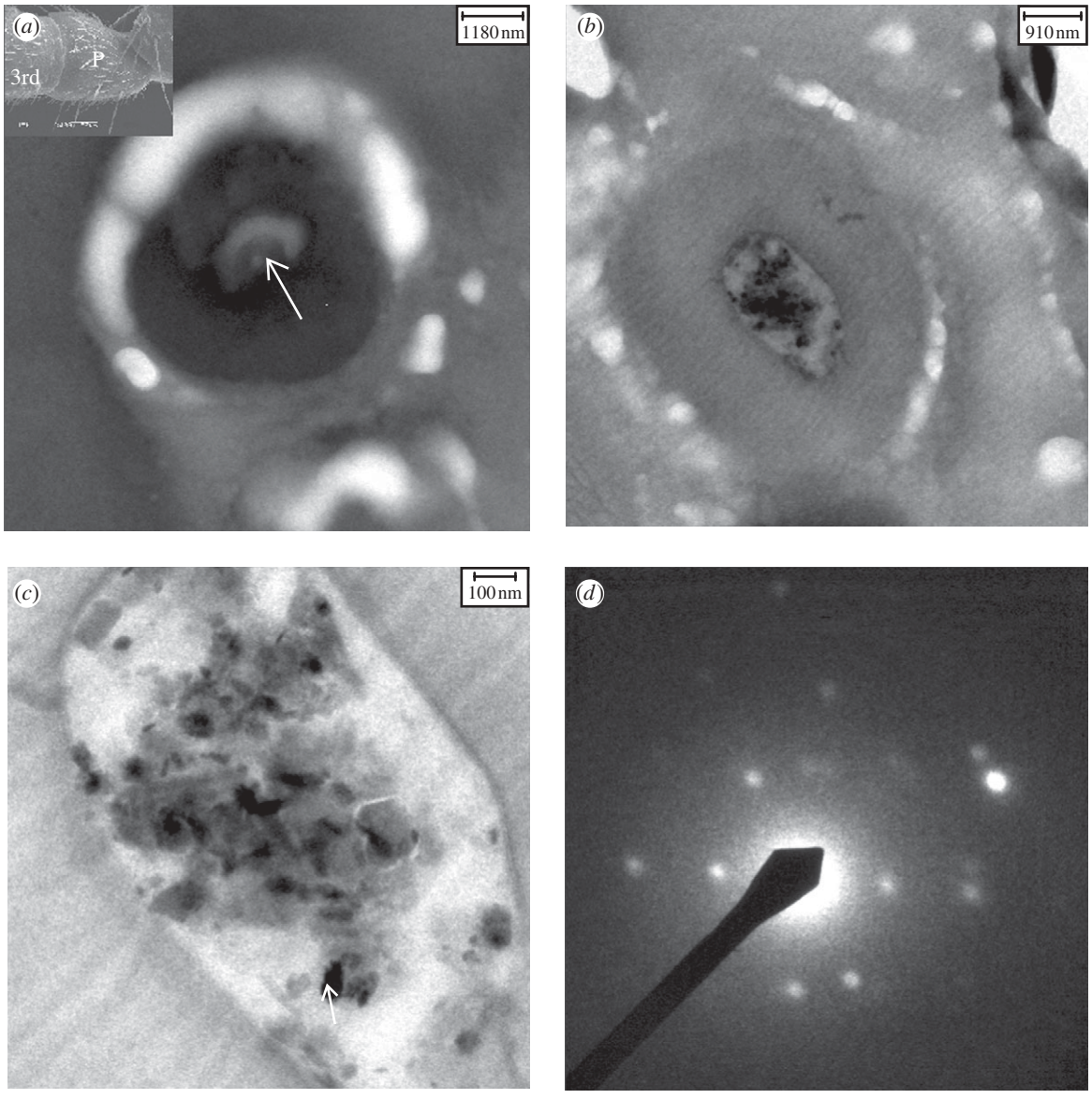

Figure 4. Transmission electron microscopy micrographs of transversal ultrathin sections of the third segment/pedicel joint cut through the antenna. (*a*) A cuticular knob (diameter, 4–5 μm). The white arrow points to a long sensory process (diameter, 1 μm). Inset: SEM of *P. marginata* antenna, showing the third segment (3rd) and the pedicel (P). (*b*) Another cuticular knob in which particles were found. (*c*) Magnified knob region in which haematite and goethite (arrow) crystals together with silicates/alumosilicates were identified. (*d*) Diffraction pattern of the goethite particle (arrow in *c*).

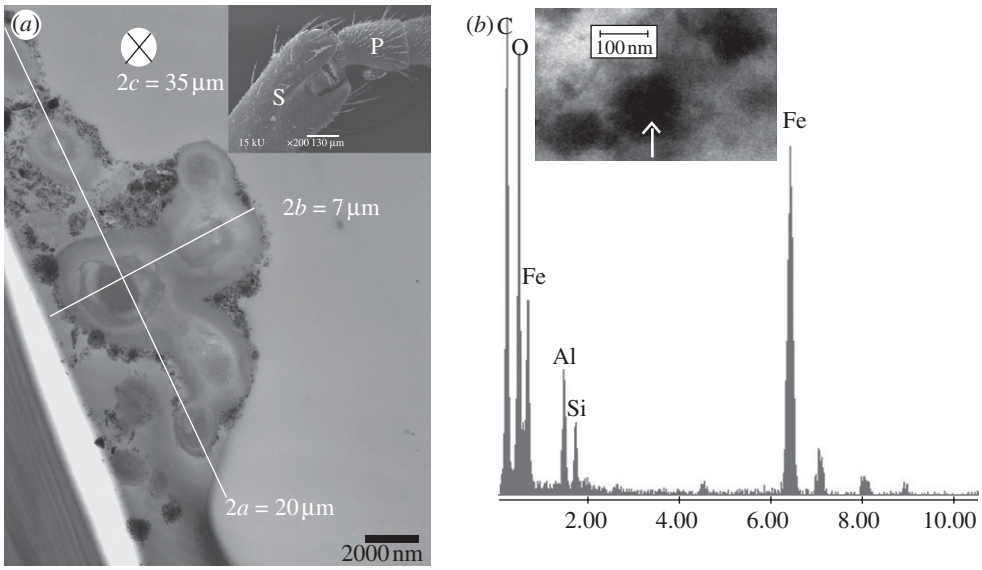

Figure 5. (*a*) Transmission electron microscopy micrograph of a transverse ultrathin section of the pedicel/scape joint showing part of the cell-like structure with particles surrounding it. The ellipsoid axes are shown. Inset: SEM image showing the joint region where the particles were found, part of the scape (S) and pedicel (P). (*b*) Energy dispersive spectroscopy spectrum of the particles in the inset (similar region of another grid) showing a high amount of iron. Inset: arrow points to a particle identified as maghaemite by its electron diffraction pattern.

observed continuously over approximately 35 µm. The three-dimensional image of this structure could be associated with an ellipsoid with an *a* semi-axis that varies from 7.5 to 12.5 µm and *b* semi-axis from 3 to 4 µm (figure 5*a*). Energy dispersive spectroscopy and SAED data were obtained and allowed us to identify haematite, goethite and magnetite/maghaemite. The arrow in the inset of figure 5*b* indicates a magnetite/maghaemite crystal.

Iron-containing areas were observed in the scape/head joint region after PB reaction (data not shown), and this result was confirmed through the diffraction patterns and EDX analysis obtained. The EDX data of the particles in this area indicated the presence of silicates/alumosilicates, Fe/O and Fe/Ti/O particles. Micrographs of ultrathin sections of these regions show a large amount of small (5–20 nm) Fe/O particles surrounding large particles (approx. 500 nm to 2 µm) of Ti/Fe/O or Fe/O (data not shown).

4. DISCUSSION

Magnetic measurements (Acosta-Avalos *et al.* 1999; Wajnberg *et al.* 2000, 2004) have suggested the presence of biogenic magnetite in the body parts (especially the antenna) of the *P. marginata* ant. In this work, TEM was used for the first time to localize and characterize iron-containing regions within antennal tissue. In magnetic extracts of head, antennae, thorax and abdomen of *P. marginata*, pure Fe/O particles were found together with Al/Si/O particles, with the latter forming the major part. But even if magnetite is present in the extracts, an unambiguous attribution to a biogenic or non-biogenic origin is not possible.

Several methods and criteria have been developed to distinguish between biotic/biogenic magnetite crystals and abiotic/non-biogenic ones, based on a wide dataset of cultured, mutant and wild-type bacteria (Guyodo *et al.* 2006; Kopp & Kirschvink 2008). Magnetite crystals (magnetosomes) synthesized intracellularly in magnetic bacteria possess unique features in terms of size, morphology and mineralogy. An identification method for magnetofossils in soils based on seven properties obtained by rock magnetic, TEM, scanning electron microscopy (SEM) and ferromagnetic resonance measurements (Kopp *et al.* 2006) was recently proposed. However, all these criteria are based on the characteristics of bacterial magnetosomes. For other organisms, it is important to keep in mind that their crystal features are not necessarily those of bacterial magnetosomes as they are supposed to be involved in the complex magnetoreception mechanism, instead of the passive magnetotactic response. Indeed, cluster arrangements of SPM instead of SD magnetite crystals were found in the upper beak skin of homing pigeons (Hanzlik *et al.* 2000). Therefore, the task of finding specific characteristics that can be unambiguously ascribed to a biological origin still remains (Fortin & Langley 2005).

Extraneous iron minerals (from the soil) can adhere to the cuticle of all body parts and/or be ingested in the thorax and abdomen. The extraction method cannot guarantee that the extraneous material is completely washed off after cleaning. Therefore, to make sure that the particles are from within the tissue and to clarify their possible physiological context, it is necessary to localize them within the tissue. The search for PB/TB reaction products under the LM is a fast screening method for regions containing Fe inside the tissue. However, as only Fe sites of the order of 1 µm can be detected under the LM, small-scale reaction products may be missing even if present. For example, we detected Fe/O crystals under the TEM, but no blue

stains were visible in the corresponding regions when observed under the LM. Moreover, in poorly fixated/infiltrated samples, a displacement of the blue dots through the reagents from their original positions may occur.

Pure Fe/O (or Fe oxides) particles were detected in different parts of the *P. marginata* antennae: third segment/pedicel, pedicel/scape and scape/head joint. These three main joints are rich in sensorial structures common to the class Insecta and open up a new aspect in iron oxide function. In the cuticular surface of scape and pedicel, there are two types of mechanoreceptors: sensilla campaniform and chaeticum (J. Ferreira de Oliveira & M. Hanzlik 2008, unpublished data). The first responds to deformations in the cuticle (Ehmer & Gronenberg 1997*a*,*b*), while the second has taste and mechanoreceptive functions (Zacharuk 1980). Moreover, on two joints, pedicel/scape and scape/head, some groups of hair plates and also sensilla campaniform were observed. The hair plate is composed of Böhm's bristles, which is a proprioceptor perceiving large changes in the antennal position (Sane *et al.* 2007) and also sensilla campaniform were observed.

Localized in the antennal pedicel, Johnston's organ functions as a mechanosensory organ, perceiving alterations of the flagellum in relation to the pedicel. It thus serves in gravireception, hearing and flight control (Sandeman 1976). This organ is composed of sensorial units called scolopidia, which are distributed symmetrically inside the pedicel. Different functions are attributed to this organ, and if the iron oxide crystals present in the cuticular knobs are somehow linked to this receptor, a magnetic function might be expected. The Johnston's organ in flies (Diptera) has been shown to be responsible for gravireception (Kamikouchi *et al.* 2009), but it is generally assumed that it lacks statoliths (Eatock 2009). Our data show that the Johnston's organ in Hymenoptera has dense mineral particles incorporated, which may well serve as statoliths in gravireception. The observed inhomogeneous distribution among the knobs is probably deceptive and caused by the unknown particle distribution in the whole three-dimensional structure. Recent papers on fruitfly (Kamikouchi *et al.* 2009; Yorozu *et al.* 2009) have shown that different clusters of neurons in this organ preferentially respond to gravity/wind, whereas others preferentially respond to sound. If the functions in the Johnston's organ are compartmentalized, the presence of particles in all knobs perhaps is not necessary. Vowles (1954) reported that the Johnston's organ is able to perceive gravity and magnetic fields that work as a stimulus for orientation in *M. ruginodis* and *M. laevinodis* ants.

In the pedicel–scape joint, a cell-like structure surrounded by different kinds of particles including iron-containing ones was found (figure 5*a*). The whole structure is assumed to be a proprioceptor because of its special location. The unknown function of this structure motivated us to test it as a magnetosensor of the geomagnetic field. The presence of magnetic particles turns the surrounding material (the outward surface) magnetizable and it represents a ferromembrane (Winklhofer 1998). Importantly, the elongated surface

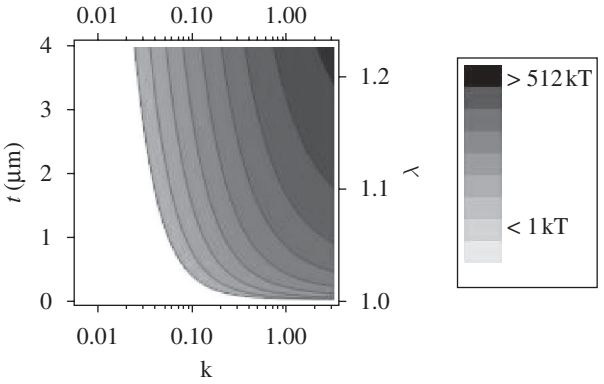

Figure 6. Magnetic torque of the ferromembrane, in units of the thermal energy, as a function of the magnetic susceptibility κ and thickness of the magnetic layer between the inner and outer ellipsoid t ($2c = 35$ μm, for theoretical modelling, $2a = 2b = 7$ μm, local geomagnetic field strength 0.3 Oe). λ is the ratio of similitude between outer and inner ellipsoid.

loaded with the magnetic particles implies that its magnetic behaviour is anisotropic, that is, it can be magnetized more easily along the long axis of the elongated structure than along the short axis (figure 5*a*). As a consequence of this magnetic anisotropy, a torque will arise if the ferromembrane is magnetized at an oblique angle with respect to the long axis. The torque tries to rotate the structure into alignment with the external magnetic field. There is no need of an actual mechanical rotation, however, in order for the proprioceptor to detect the torque. The magnetic torque acting on the proprioceptor will bias the mechanical torques (for example, owing to movement of the filaments), and by comparing the output of a magnetically coated proprioceptor with a non-magnetic adjacent one, the magnetic torque can be isolated. This is conceptually similar to the magnetite null detector suggested by Edmonds (1992), who considered the torque balance between hypothetical magnetite-loaded hair cell detectors and non-magnetic ones. The derivation of our theoretical model can be found in appendix A. To provide a quantitative assessment of the magnetic field sensitivity of the ferromembrane, we have to make an assumption about the intrinsic low-field magnetic susceptibility κ, which depends on the size and concentration of the magnetic particles in the shell as well as on the intrinsic magnetic parameters of the particles. Nanocrystalline haematite particles, as can be observed in figure 3*a*, are often found to be SPM, for which low-field magnetic susceptibilities may be up to 0.01 G/Oe (Bødker *et al.* 1994; Raming *et al.* 2002). For a magnetic shell of average thickness of approximately 2.5 μm ($\lambda = 1.075$; appendix A) and intrinsic low-field susceptibility of $\kappa = 0.03$, the torque is just enough to balance the thermal energy at room temperature (figure 6). This is a worst-case scenario, which does not involve the possibility of using strongly ferromagnetic compounds such as maghaemite or magnetite (figure 5*b* inset) as well. A small amount of 5 per cent incorporated with either component would significantly amplify the torque.

In ants, the scape is connected to the head by a ball joint. It can be moved by four extrinsic muscles, two

levator and two depressor muscles, which are located within the head capsule. This gives the scape, and hence the entire antenna, a large freedom of movement. The second antennal segment, the pedicel, is connected to the scape by a hinge joint. It can only be moved in a single plane by a pair of muscles confined within the scape and referred to as intrinsic antennal muscles. All these muscles together control antennal movements, ranging from slow position-maintaining tasks to fast antennal flicks (Ehmer & Gronenberg 1997*a*,*b*). Within the head capsule, the Janet's organ is found. Scolopales and dendrites, which compose this organ, together form an elastic ribbon that is stretched by antennal movement. One end of the scolopale inserts at internal processes at the basis of the scape (Ehmer & Gronenberg 1997*a*,*b*). The iron-containing particles found inside the ball joint and surrounding regions suggest that this part can also be involved, together with other structures, in the detection of the Earth's magnetic field.

The presence of magnetic particles found within the tissue close to mechanosensitive structures in very specific areas along the antenna parts, probably incorporated during the growing process, suggests a possible magnetoreception function.

J. F. d. O. thanks Dr Marcos Farina (Anatomy Department/UFRJ, Rio de Janeiro, Brazil) for the use of the Biomineralization Lab facilities for sample preparation and Fernando Pereira de Almeida for helping in the first sample preparation. J. F. d. O. was funded by a scholarship from CNPq (from April 2007 to March 2008; process 290098/2006-8) and by the Human Frontier Science Program, HFSP grant RGP 28/2007 (from April 2008 to June 2008). M. W. acknowledges funding from the Deutsche Forschungsgemeinschaft (DFG grant Wi1828/4).

APPENDIX A

A.1. Magnetic torque experienced by a ferromembrane in an external magnetic field

To derive an expression for the magnetic torque, we assume that the ferromembrane has homogeneous magnetic susceptibility and that its shape can be approximated by a prolate ellipsoidal shell. The magnetic energy W of a homogeneously magnetized shell confined by two confocal ellipsoids is given by:

$$W = -\frac{1}{2} M H_0 V, \tag{A 1}$$

where M is the magnetization, H_0 the external field strength (in Oe) and V the volume of the shell, given by $V = 4\pi/3\ (\lambda^3 - 1)\ c^3\ (1 - \varepsilon^2)$, where $\varepsilon^2 = 1 - (a/c)^2$ and $\lambda > 1$ is the ratio of similitude between the inner ellipsoid (c, a) and the outer ellipsoid ($c_1 = \lambda c$, $a_1 = \lambda a$). Equation (A 1) can be rewritten as

$$W = \frac{1}{2}(\kappa'_c \cos^2\theta + \kappa'_a \sin^2\theta) H_0^2 V, \tag{A 2}$$

where θ is the polar angle of the external magnetic field axis with respect to the long axis of the body and κ'_c and κ'_a are the apparent susceptibilities along the long and short axes of either ellipsoid, respectively, with

$$\kappa'_\nu = \frac{\kappa}{(1 + N_\nu \kappa)}, \quad (\nu = a, c), \tag{A 3}$$

where κ is the intrinsic magnetic susceptibility and N_c, the geometric demagnetizing factor along the long axis, is given as

$$\frac{N_c}{4\pi} = \frac{1 - \varepsilon^2}{\varepsilon^3}(\mathrm{Artanh}(\varepsilon) - \varepsilon) \tag{A 4}$$

(e.g. Osborn 1945; Stoner 1945), and $N_a = N_b = (4\pi - N_c)/2$. The magnetically coated structure described in the article has a long axis $2c = 35\ \mu$m and short axes $2a \approx 2b = 7\ \mu$m. For $a/c = 3.5/17.5$ ($\varepsilon^2 = 0.96$), $N_c = 0.70$ and $N_a = 5.93$. From equation (A 2), we obtain the torque as

$$T = \frac{\mathrm{d}W}{\mathrm{d}\theta} = \frac{1}{2}(\kappa'_c - \kappa'_a) \sin 2\theta H_0^2 V. \tag{A 5}$$

The sin 2θ dependence of T implies an axial field response (figure 7), as can be expected for an SPM system.

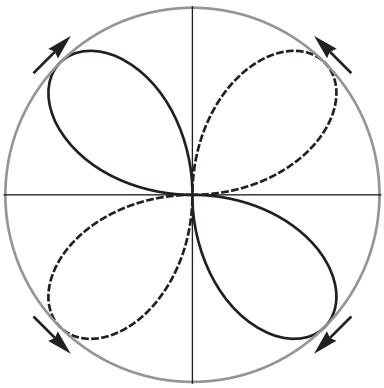

Figure 7. Polar plot of torque distribution in the θ plane. θ is the angular orientation of the magnetic field axis relative to that of the long axis of the ellipsoidal magnetic shell (vertical). The lines of the clubs represent clockwise (solid) and counterclockwise (dotted) sense of torque, respectively (see arrows). The node lines 0° (up) and 180° (down) represent stable orientation (converging arrows), and the node lines 90° and 270° are related to labile orientation (diverging arrows).

REFERENCES

Acosta-Avalos, D., Wajnberg, E., Oliveira, P. S., Leal, I., Farina, M. & Esquivel, D. M. S. 1999 Isolation of magnetic nanoparticles from *Pachycondyla marginata* ants. *J. Exp. Biol.* **202**, 2687–2692.

Acosta-Avalos, D., Esquivel, D. M. S., Wajnberg, E., Lins de Barros, H. G. P., Oliveira, P. S. & Leal, I. 2001 Seasonal patterns in the orientation system of the migratory ant *Pachycondyla marginata*. *Naturwissenschaften* **88**, 343–346. (doi:10.1007/s001140100245)

American Mineralogist Crystal Structure Database. See http://rruff.geo.arizona.edu/AMS/result.php.

Anderson, J. B. & Vander Meer, R. K. 1993 Magnetic orientation in fire ant, *Solenopsis invicta*. *Naturwissenschaften* **80**, 568–570. (doi:10.1007/BF01149274)

Blakemore, R. P. 1975 Magnetotactic bacteria. *Science* **190**, 377–379. (doi:10.1126/science.170679)

Bødker, F. S., Mørup, S. & Linderoth, S. 1994 Surface effects in metallic iron nanoparticles. *Phys. Rev. Lett.* **72**, 282–285. (doi:10.1103/PhysRevLett.72.282).

Çamlitepe, Y. & Stradling, D. J. 1995 Wood ants orient to magnetic fields. *Proc. R. Soc. Lond. B* **261**, 37–41. (doi:10.1098/rspb.1995.0114).

Çamlitepe, Y., Aksoy, V., Uren, N., Yilmaz, A. & Becenen, I. 2005 An experimental analysis on the magnetic field sensitivity of the black-meadow ant *Formica pratensis* Retzius (Hymenoptera: Formicidae). *Acta Biol. Hung.* **56**, (doi:10.1556/ABiol.56.2005.3-4.5)

Davila, A. F., Fleissner, G., Winklhofer, M. & Petersen, N. 2003 A new model for a magnetoreceptor in homing pigeons based on interacting clusters of superparamagnetic magnetite. *Phys. Chem. Earth* **28**, 647–652. (doi:10.1016/S1474-7065(03)00118-9)

Davila, A. F., Winklhofer, M., Shcherbakov, V. P. & Petersen, N. 2005 Magnetic pulse affects a putative magnetoreceptor mechanism. *Biophys. J.* **89**, 56–63. (doi:10.1529/biophysj.104.049346)

Diebel, C. E., Proksch, R., Green, C. R., Nellson, P. & Walker, M. M. 2000 Magnetite defines a vertebrate magnetoreceptor. *Nature* **406**, 299–302. (doi:10.1038/35018561).

Eatock, R. A. 2009 Up, down, flying around. *Nature* **458**, 156–157. (doi:10.1038/458156a)

Edmonds, D. T. 1992 A magnetite null detector as the migrating bird's compass. *Proc. Biol. Sci.* **249**, 27–31. (doi:10.1098/rspb.1992.0079)

Ehmer, B. & Gronenberg, W. 1997*a* Antennal muscles and fast antennal movements in ants. *J. Comp. Physiol. B* **167**, 287–296. (doi:10.1007/s003600050076)

Ehmer, B. & Gronenberg, W. 1997*b* Proprioceptors and fast antennal reflexes in the ant *Odontomachus* (Formicidae, Ponerinae). *Cell Tissue Res.* **290**, 153–165. (doi:10.1007/s004410050917)

Ferreira, J., Cernicchiaro, G., Winklhofer, M., Dutra, H., Oliveira, P. S., Esquivel, D. M. S. & Wajnberg, E. 2005 Comparative magnetic measurements on social insects. *J. Magn. Magn. Mater.* **289**, 442–444. (doi:10.1016/j.jmmm.2004.11.124)

Fleissner, G., Holtkamp-Rotzler, E., Hanzlik, M., Winklhofer, M., Fleissner, G., Petersen, N. & Wiltschko, W. 2003 Ultrastructural analysis of a putative magnetoreceptor in the beak of homing pigeons. *J. Comp. Neurol.* **458**, 350–360. (doi:10.1002/cne.10579)

Fortin, D. & Langley, S. 2005 Formation and occurrence of biogenic iron-rich minerals. *Earth Sci. Rev.* **72**, 1–19. (doi:10.1016/j.earscirev.2005.03.002)

Gould, J. L. 2008 Animal navigation: the evolution of magnetic orientation. *Curr. Biol.* **18**, R482–R484. (doi:10.1016/j.cub.2008.03.052)

Gould, J. L., Kirschvink, J. L. & Deffeyes, K. S. 1978 Bees have magnetic remanence. *Science* **201**, 1026–1028. (doi:10.1126/science.201.4360.1026)

Guyodo, Y., LaPara, T. M., Anschutz, A. J., Lee Penn, R., Banerjee, S. K., Geiss, C. E. & Zanner, W. 2006 Rock magnetic, chemical and bacterial community analysis of a modern soil from Nebraska. *Earth Planet. Sci. Lett.* **251**, 1–2. (doi:10.1016/j.epsl.2006.09.005)

Hallberg, E. 1981 Johnston's organ in *Neodiprion sertifer* (Insecta: Hymenoptera). *J. Morphol.* **167**, 305–312. (doi:10.1002/jmor.1051670305)

Hanzlik, M., Heunemann, C., Holtkamp-Rötzler, E., Winklhofer, M., Petersen, N. & Fleissner, G. 2000 Superparamagnetic magnetite in the upper beak tissue of homing pigeons. *Biometals* **13**, 325–331. (doi:10.1023/A:1009214526685)

Hsu, C. Y., Ko, F. Y., Li, C. W., Fann, K. & Lue, J. T. 2007 Magnetoreception system in honeybees (*Apis mellifera*). *PLoS ONE* **2**, e395–e406. (doi:10.1371/journal.pone.0000395)

Kamikouchi, A., Inagaki, H. K., Effertz, T., Hendrich, O., Fiala, A., Goepfert, M. C. & Ito, K. 2009 The neural basis of *Drosophila* gravity—sensing and hearing. *Nature* **458**, 165–171. (doi:10.1038/nature07810)

Kirschvink, J. L. & Gould, J. L. 1981 Biogenic magnetite as a basis for magnetic field detection in animals. *Biosystems* **13**, 181–201. (doi:10.1016/0303-2647(81)90060-5)

Kopp, R. E. & Kirschvink, J. L. 2008 The identification and biogeochemical interpretation of fossil magnetotactic bacteria. *Earth Sci. Rev.* **86**, 42–61. (doi:10.1016/j.earscirev.2007.08.001)

Kopp, R. E., Nash, C. Z., Kobayashi, A., Weiss, B. P., Bazylinski, D. A. & Kirschvink, J. L. 2006 Ferromagnetic resonance spectroscopy for assessment of magnetic anisotropy and magnetostatic interactions: a case study of mutant magnetotactic bacteria. *J. Geophys. Res.* **111**, B12S25(11–15). (doi:10.1029/2006JB004529)

Lohmann, K. J., Lohmann, C. M. F. & Endres, C. S. 2008 The sensory ecology of ocean navigation. *J. Exp. Biol.* **211**, 1719–1728. (doi:10.1242/jeb.015792)

Maeda, K., Henbest, K. B., Cintolesi, F., Kuprov, I., Rodgers, C. T., Liddell, P. A., Gust, D., Timmel, C. R. & Hore, P. J. 2008 Chemical compass model of avian magnetoreception. *Nature*, 387–391. (doi:10.1038/nature06834)

Mann, S., Sparks, N. H. C., Walker, M. M. & Kirschvink, J. L. 1988 Ultrastructure, morphology and organization of biogenic magnetite from sockeye salmon, *Oncorhynchus nerka*: implications for magnetoreception. *J. Exp. Biol.* **140**, 35–49.

Masson, C. & Gabouriaut, D. 1973 Ultrastructure de l'organe de Johnston de la Fourmi *Camponotus vagus* Scop. (Hymenoptera, Formicidae). *Z. Zellforsch. Mikrosk. Anat.* **140**, 39–75. (doi:10.1007/BF00307058)

O'Leary, D. P., Vilches-Troya, J., Dunn, R. F. & Campos-Munoz, A. 1981 Magnets in guitarfish vestibular receptors. *Experientia* **37**, 86–88. (doi:10.1007/BF01965587)

Osborn, J. A. 1945 Demagnetizing factors for the general ellipsoid. *Phys. Rev.* **67**, 351–357. (doi:10.1103/PhysRev.67.351)

Raming, T. P., Winnubst, A. J. A., van Kats, C. M. & Philipse, A. P. 2002 The synthesis and magnetic properties of nanosized hematite (α-Fe2O3) particles. *J. Colloid Interface Sci.* **249**, 346–350. (doi:10.1006/jcis.2001.8194)

Ritz, T., Adem, S. & Schulten, K. 2000 A model for photoreceptor-based magnetoreception in birds. *Biophys. J.* **78**, 707–718. (doi:10.1016/S0006-3495(00)76629-X)

Ritz, T., Thalau, P., Phillips, J., Wiltschko, R. & Wiltschko, W. 2004 Resonance effects indicate a radical pair mechanism for avian magnetic compass. *Nature* **429**, 177–180. (doi:10.1038/nature02534)

Riveros, A. J. & Srygley, R. B. 2008 Do leafcutter ants, *Atta colombica*, orient their path-integrated home vector with a magnetic compass? *Anim. Behav.* **75**, 1273–1281. (doi:10.1016/j.anbehav.2007.09.030)

Sandeman, D. C. 1976 *Structure and function of proprioceptors in the invertebrates*. London, UK: Chapman & Hall.

Sane, S. P., Dieudonné, A., Willis, M. A. & Daniel, T. L. 2007 Antennal mechanosensors mediate flight control in moths. *Science* **315**, 863–866. (doi:10.1126/science.1133598)

Shcherbakov, V. P. & Winklhofer, M. 1999 The osmotic magnetometer: a new model for magnetite-based magnetoreceptors in animals. *Eur. Biophys. J.* **28**, 380–392. (doi:10.1007/s002490050222)

Stoner, E. C. 1945 The demagnetizing factors for ellipsoids. *Phil. Mag.* **36**, 803–821.

Tsujiuchi, S., Sivan-Loukianova, E., Eberl, D. F., Kitagawa, Y. & Kadowaki, T. 2007 Dynamic range compression in the honey bee auditory system toward waggle dance sounds. *PLoS ONE* **2**, e234–e244. (doi:10.1371/journal.pone.0000234)

Vacha, M. 1997 Magnetic orientation in insects. *Biologia* **52**, 629–636.

Vilches-Troya, J., Dunn, R. F. & O'Leary, D. P. 1984 Relationship of the vestibular hair cells to magnetic particles in the otolith of the guitarfish sacculus. *J. Comp. Neurol.* **226**, 489–494. (doi:10.1002/cne.902260404)

Vowles, D. M. 1954 The orientation of ants II. Orientation to light, gravity and polarized light. *J. Exp. Biol.* **31**, 356–375.

Wajnberg, E., Acosta-Avalos, D., El-Jaick, L. J., Abraçado, L., Coelho, J. L. A., Bazukis, A. F., Morais, P. C. & Esquivel, D. M. S. 2000 Electron paramagnetic resonance study of the migratory ant *Pachycondyla marginata* abdomens. *Biophys. J.* **78**, 1018–1023. (doi:10.1016/S0006-3495(00)76660-4)

Wajnberg, E., Cernicchiaro, G. R. & Esquivel, D. M. S. 2004 Antennae: the strongest magnetic part of the migratory ant. *Biometals* **17**, 467–470. (doi:10.1023/B:BIOM.0000029443.93732.62)

Walker, M. M., Diebel, C. E., Haugh, C. V., Pankhurst, P. M., Montgomery, J. C. & Green, C. R. 1997 Structure and function of the vertebrate magnetic sense. *Nature* **390**, 371–376. (doi:10.1038/37057)

Wiltschko, W. & Wiltschko, R. 1995 *Magnetic orientation in animals*. Berlin, Germany: Springer Verlag.

Wiltschko, R., Munro, U., Ford, H., Stapput, K. & Wiltschko, W. 2008 Light-dependent magnetoreception: orientation behaviour of migratory birds under dim red light. *J. Exp. Biol.* **211**, 3344–3350. (doi:10.1242/jeb.020313)

Winklhofer, M. 1998 *Modelle hypothetischer Magnetfeldrezeptoren auf der Grundlage biogenen Magnetits*. Munich, Germany: Ludwig–Maximilians-Universität.

Yorozu, S., Wong, A., Fischer, B. J., Dankert, H., Kernan, M. J., Kamikouchi, A., Ito, K. & Anderson, D. J. 2009 Distinct sensory representations of wind and near-field sound in the *Drosophila* brain. *Nature* **458**, 200–205. (doi:10.1038/nature07843)

Zacharuk, R. Y. 1980 Ultrastructure and function of insect chemosensilla. *Annu. Rev. Entomol.* **25**, 27–47. (doi:10.1146/annurev.en.25.010180.000331)